Contributed paper

OPTO-ELECTRONICS REVIEW 11(4), 261–267 (2003)

Electron traps in $Cu(In,Ga)Se_2$ absorbers of thin film solar cells studied by junction capacitance techniques

M. IGALSON* and P. ZABIEROWSKI

Faculty of Physics, Warsaw University of Technology
75 Koszykowa Str., 00–662 Warszawa, Poland

The results of steady state and transient capacitance spectroscopy for ZnO/CdS/Cu(In,Ga)Se_2 solar cells are presented. A minority carrier signal from the interface region of absorber has been investigated using Laplace-DLTS. Contributions belonging to three discrete electron traps with thermal emission rates distorted by electric field-assisted tunnelling have been identified and assigned to In_{Cu} antisite defect. Support for these conclusions has been also provided by admittance spectroscopy of samples in various metastable states created by prolonged exposition to light, voltage bias or elevated temperature. Two other deep electron traps have been revealed by the use of DLTS injection. One of them, tentatively assigned to the V_{Se} defect, is involved in the metastable phenomena observed in Cu(In,Ga)Se_2 – based solar cells. Judging from the high value of capture cross section for carriers of both signs we conclude that it might be a dominating recombination centre in these devices.

Keywords: solar cells, Cu(In,Ga)Se_2, defect levels, DLTS, admittance spectroscopy.

1. Introduction

Thin film heterojunction solar cells based on Cu(In,Ga)Se_2 (CIGS) absorber hold now record efficiency among all thin film structures (18.9%, NREL) [1]. However, fundamental knowledge about this material and in particular about electronic properties of defects is still far from being satisfactory. In order to push further the limits of efficiency and also to introduce novel, cheaper technologies, better understanding of defect physics in CIGS seems to be indispensable. In this paper we summarize our findings on that subject.

We use steady state capacitance spectroscopy (admittance spectroscopy) and several variations of transient capacitance spectroscopy DLTS to obtain information on electronic parameters of deep defects in CIGS. The interpretation of the capacitance spectroscopy data is often complicated not only because of the complexity of the structure. An important feature of these cells is a presence of metastable phenomena, i.e., persistent changes of electrical characteristics induced by prolonged illumination, voltage bias, and annealing at elevated temperatures [2–5]. These effects are also observed in the DLTS and admittance spectra, so in the designing of the experiment and in interpretation of the results they have to be taken into account.

The devices studied in this work are solar cells of standard configuration and well-established baseline fabrication process prepared in Ångström Solar Centre, Uppsala University [6] and Institute of Physical Electronic, Stuttgart University [7]. CIGS absorber has been deposited by co-evaporation on molybdenum-covered soda-lime glass. Then follows CdS buffer obtained by chemical bath deposition and sputtered ZnO window (80 nm of i-ZnO and about 300 nm of ZnO:In). The structure is completed by evaporation of an aluminium grid. Photovoltaic conversion efficiencies of these devices without antireflection coating are usually about 14%.

2. Experimental methods

2.1. DLTS

Deep level transient spectroscopy (DLTS) is based on a fact that capacitance of the junction depends on the total charge in the depletion region. When traps are filled by voltage pulse the capacitance of the junction increases if the minority carriers are captured and decreases in case of majority carriers. After removal of the pulse a transient C(t) might be observed

$$\Delta C/C \propto N_T/N_a \exp\{-e_T t\}. \quad (1)$$

The decay rate e_T corresponds to the thermal emission rate of trapped carriers

$$e_T = N_{c,v} v_{th} \sigma_{e,h} \exp\{-E_T/kT\}, \quad (2)$$

where v_{th} is the thermal velocity, $\sigma_{e,h}$ is the capture cross section for electrons or holes, and $N_{c,v}$ is the density of

*e-mail: igalson@if.pw.edu.pl

states in the conduction or valence band. The transient is processed by electronic filter in the DLTS apparatus. When the time constant of the transient for a given temperature fits to a prefixed "emission rate window", a maximum of the DLTS signal is observed and hence the emission rate at the given temperature is determined. Electronic parameters of the trap level under investigation are derived from the Arrhenius plot of the emission rates measured at various temperatures [8].

The DLTS measurements shown in this work have been made at a constant temperature in a frequency scan mode: the filling pulses have been generated with frequency changing quasi-continuously from 0.5 Hz to 2500 Hz. With rectangular weighting function and lock-in type averaging used in our DLTS apparatus (DLS-E82), the maximum of the DLTS output arises at a pulse frequency corresponding to the half of emission rate from the trap level.

In the standard DLTS method, the junction is held at reverse quiescent bias and filling pulses are applied in forward direction. A variation of standard DLTS is a reverse bias DLTS (RDLTS), in which a pulse in the reverse direction is superimposed on the quiescent bias [9]. Here a capture process is analysed by the DLTS electronic filter, but since the traps situated at the cross-point of the Fermi-level and trap level provide maximum contribution to the capacitance transient, capture rate measured in the RDLTS experiment is equal to the emission rate. It has been shown that this type of measurement is an efficient tool for analysis of the electron traps in the region at or close to the interface [3,10].

Another method employed in this work is Laplace-DLTS [11]. Here full capacitance transient is registered and then numerically analysed. Calculation of the inverse Laplace transformation of $C(t)$ by using a general expression describing capacitance transient,

$$C(t) = \int g(E)\exp\{-e_T(E)t\}dE, \tag{3}$$

is performed. That method gives much higher resolution than standard DLTS. Calculations give sharp peaks at frequencies corresponding to the emission rates from discrete levels.

2.2. Admittance spectroscopy

Admittance spectroscopy is based on measurements of capacitance of the structure as a function of modulating ac voltage frequency and temperature [12]. In the limit of high frequency/low temperature only shallow levels contribute to the capacitance, which in that case corresponds to the total depletion width W of the device

$$C_{high} = \frac{\varepsilon\varepsilon_o}{W}, \tag{4}$$

Trap levels of the concentration N_T contribute to the capacitance of the junction if they are able to respond to the ac signal, i.e., if their emission rate e_T is higher than the ac frequency. Thus, if $e_T \ll \omega$, capacitance is given by the expression.

$$C_{low} = \frac{\varepsilon\varepsilon_o}{W}\left(1 + \frac{N_T(W - x_T)}{N_a W + x_T N_T}\right). \tag{5}$$

Here x_T is the distance between the interface and a crossing point of the Fermi-level and a trap level (see Fig. 1) and N_a is the net acceptor concentration. Thus, in the dependence of $C(\omega)$ a transition step from low frequency to high frequency conditions at the angular frequency of $\omega_o = 2e_T$ is observed.

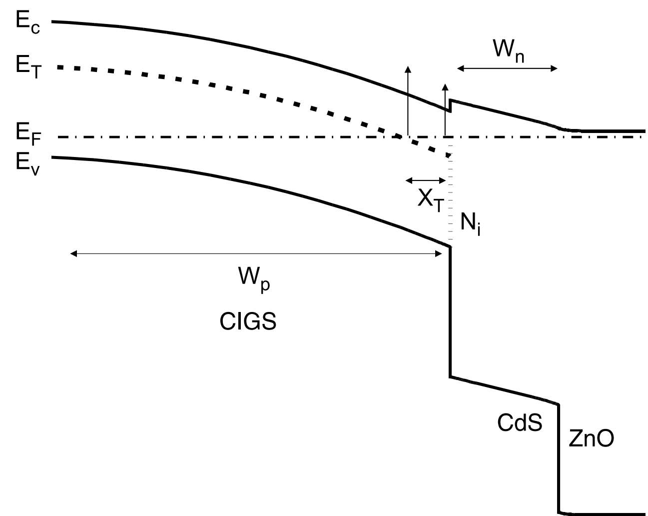

Fig. 1. Band diagram of ZnO/CdS/CIGS heterojunction. Thermal excitation processes from discrete bulk level and interface levels are shown.

Interface states in the heterojunction may also respond to the ac signal [13,14]. For electron-type traps with continuous energetical distribution at interface high frequency capacitance corresponds to the total depletion width

$$C_{high} = \frac{\varepsilon\varepsilon_o}{W_n} + \frac{\varepsilon\varepsilon_o}{W_p}, \tag{6}$$

while at low frequency the width of the p-type layer is obtained

$$C_{low} = \frac{\varepsilon\varepsilon_o}{W_p}. \tag{7}$$

Activation energy of the emission rate is here related to the distance of the Fermi-level position at the interface to the conduction band edge (see Fig. 1)

$$E_T = E_C - E_F \tag{8}$$

 © 2003 COSiW SEP, Warsaw

In this paper we will present the admittance spectra as a function $W(\omega) = \varepsilon\varepsilon_o/C(\omega)$. A plot of $d(W)/d(\ln\omega)$ vs. frequency displays a maximum at ω_o. When bulk levels are responsible for a step, the height of this maximum depends on the traps concentration and is equal to

$$\left.\frac{dW}{d(\ln\omega)}\right|_{\omega=\omega_o} = \frac{N_T(W - x_T)}{2(N_a - N_T)}. \quad (9)$$

When the signal belongs to the interface states it amounts to

$$\left.\frac{dW}{d(\ln\omega)}\right|_{\omega=\omega_o} = \frac{W_n}{2}. \quad (10)$$

3. Donor traps in the interface region

In the reverse bias DLTS and admittance spectrum of baseline devices an electron trap level is commonly detected in the low temperature region. Apparent position of that level varies somewhat from sample to sample and depends also on the history of the sample. Annealing at elevated temperature, prolonged illumination, or applying voltage bias induce persistent changes in the apparent level depth derived from admittance and RDLTS experiments. Thus, this signal has been interpreted as due to the continuous spectrum of donor-type electron levels at the interface [13,14]. Changes of the energy within this model can be explained by the changes of the Fermi-level position at the interface (Eq. 8) induced by the persistent changes of the charge distribution within the junction.

However, a detailed investigation performed by use of the reverse-bias DLTS with Laplace transform analysis provided alternative explanation. High spectral resolution of Laplace-DLTS allowed to distinguish, in the signal, more than one level which might appear or disappear from the spectrum depending on the state of the sample (annealed, light-soaked) [15,16]. In Fig. 2, the examples of the Laplace-RDLTS spectra, featuring one or two levels depending on the state of the sample, are shown. It has been concluded that discrete bulk levels are involved in the emission. It has been also observed that the Arrhenius plots of the emission rates are highly non-linear which suggests a significant contribution of tunnelling to thermal emission. Therefore simple Eq. (2) for thermal emission rate from the trap level has to be replaced by

$$e_{TAT} = e_T\left(1 + \int_0^{E_T/kT} \exp\left(z - z^{\frac{3}{2}}\left(\frac{4}{3}\frac{(2m^*)^{\frac{1}{2}}(kT)^{\frac{3}{2}}}{q\hbar F}\right)\right)dz\right). \quad (11)$$

In this formula, a contribution of thermally assisted tunnelling of electrons from a trap to the conduction band, facilitated by a presence of high electric field F in the region close to the interface, has been included [17,18]. In order to derive the trap parameters, a multidimensional fit of the highly nonlinear Eq. (11) to the experimental data has been performed. For this purpose we used a method of the minimization of the chi-square function along coordinate directions. As error estimates on the best-fit parameters (electric field, activation energy and capture cross section) we took the confidence limits calculated as the constant chi-square boundaries: $\Delta\chi^2 = \chi^2 - \chi^2_{\min} = K_\beta$. The value of $K_\beta = 3.5$ was chosen to ensure the confidence level β to be above 0.9.

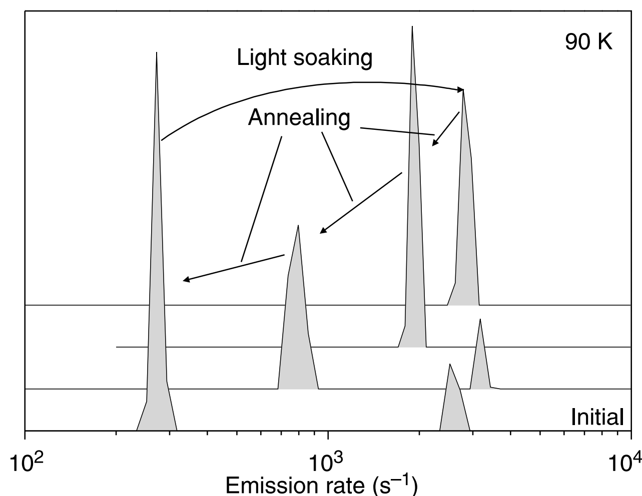

Fig. 2. Spectra of Laplace-RDLTS obtained for the cell in various persistent states: initial, after light soaking at room temperature, and after several annealing steps.

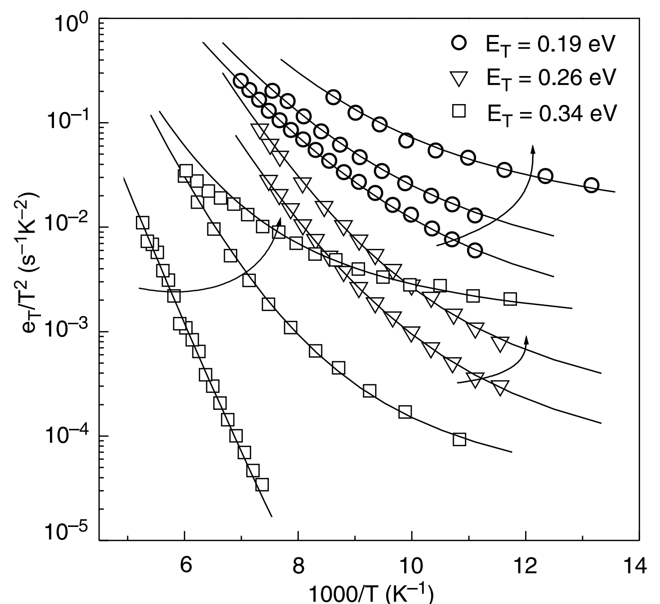

Fig. 3. Arrhenius plots of emission rates derived from Laplace-RDLTS for various samples and in various states together with best fit curves calculated by use of Eq. (11). Best fit have been obtained for thermal activation energies specified in the picture and increasing strengths of the electric field indicated by arrows.

Table 1. Electronic parameters of deep traps derived from capacitance spectroscopy. In the last column are given suggested level assignments and theoretical values of thermal ionisation energies (after Refs. 19 and 23).

Electrical activity	$E_C - E_T$ (eV)	$E_T–E_V$ (eV)	σ_p (cm^2)	σ_n (cm^2)	Defect
Donor	0.19			6×10^{-17}	$(In_{Cu} + V_{Cu})^+$ (E_c – 0.20 eV)
Donor	0.26			4×10^{-16}	In_{Cu}^+ (E_c – 0.26 eV)
Donor	0.34			4×10^{-15}	In_{Cu}^{++} (E_c – 0.34 eV)
Donor	0.47		$< 10^{-18}$	5×10^{-16}	O_{Se}?
Donor	> 0.6		5×10^{-14}	$> 5\times10^{-14}$	V_{Se}^0 (E_c – 0.1 eV relaxed, E_v + 0.1 eV without relaxation)

Fitting of the Eq. (11) to the Laplace-RDLTS data collected for many samples in the relaxed and in the metastable states induced by light or voltage bias has been performed. The examples of the Arrhenius plots of emission rates and theoretical fits are shown in Fig. 3. These results prove that "interface level" it is in fact one of the three discrete donor-type traps with emission rates modified by the electric field-enhanced tunnelling. Comparing the activation energies obtained from the fits to the theoretical energy levels calculated for intrinsic defects in CIGS [19] we have concluded that these traps belong to In_{Cu} antisite (see Table 1). As illustrated in Fig. 4, it depends on the position of Fermi-level in the vicinity of interface which level is observed in the experiment. In the case of double defect In_{Cu} one may notice that as long as the Fermi-level is above both levels, only shallower level (0/+) is occupied, while if the Fermi level is in-between both levels, only emission from (+/++) state might be observed. The changes of the admittance and RDLTS spectra induced by light or voltage bias might then be explained by two factors: changes of the Fermi-level position and the electric field strength in the vicinity of interface.

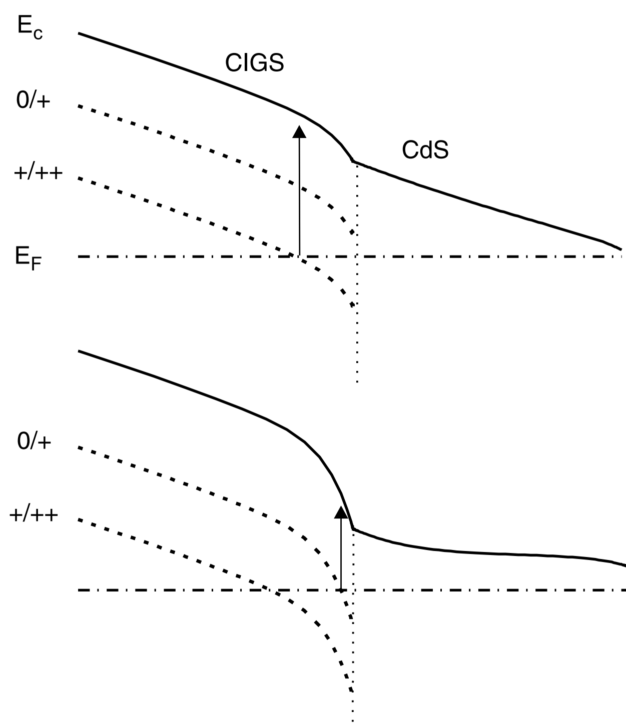

Fig. 4. Band diagram of the junction interface region with a double donor. Possible excitation processes depending on the position of the Fermi-level are shown.

This interpretation of the source of the RDLTS peak has been confirmed by the admittance measurements [5]. They show that the difference between depletion widths in the high and low frequency limit exceeds in many instances the maximum width of the depleted n-type region of the structure (0.13 mm in our devices) which is expected in case of interface traps (Eq. 6 and 7). This is illustrated in Fig. 5, a derivative of the admittance spectrum after reverse-bias soaking features a peak of magnitude exceeding significantly $1/2W_n$. Moreover, the experiments with reverse-bias soaking at elevated temperatures prove that in some cases we could observe two levels clearly belonging to two different defects associated with In_{Cu} antisite. An example is shown in Fig. 6 where the Arrhenius plots of the emission rates derived from admittance spectroscopy are compared for samples featuring different levels in the relaxed state. In one sample after reverse-bias soaking at 330 K, the initial emission [presumably from In_{Cu} (0/+)] is entirely replaced by the emission from In_{Cu} (+/++). In the other, initially the emission from the 0.19 eV level is observed and after reverse-bias the same as in the first sample In_{Cu} (++/+) level appears in addition to still present level 0.19 eV. It is worth noticing also that the In_{Cu} (++/+) level has been also observed in the relaxed state of the sodium-free device (fabricated on the glass substrate covered with SiO_2 barrier) [16].

4. Midgap electron traps

Levels most detrimental for the performance of solar cells are deep midgap minority carrier traps with large capture cross sections for both minority and majority carriers. Therefore we have paid special attention to identification of these levels in the CIGS absorbers.

DLTS measurements by use of injection pulses, which should fill deep minority carrier traps, do not show any thermally activated signal up to 360 K in the efficient base-

 © 2003 COSiW SEP, Warsaw

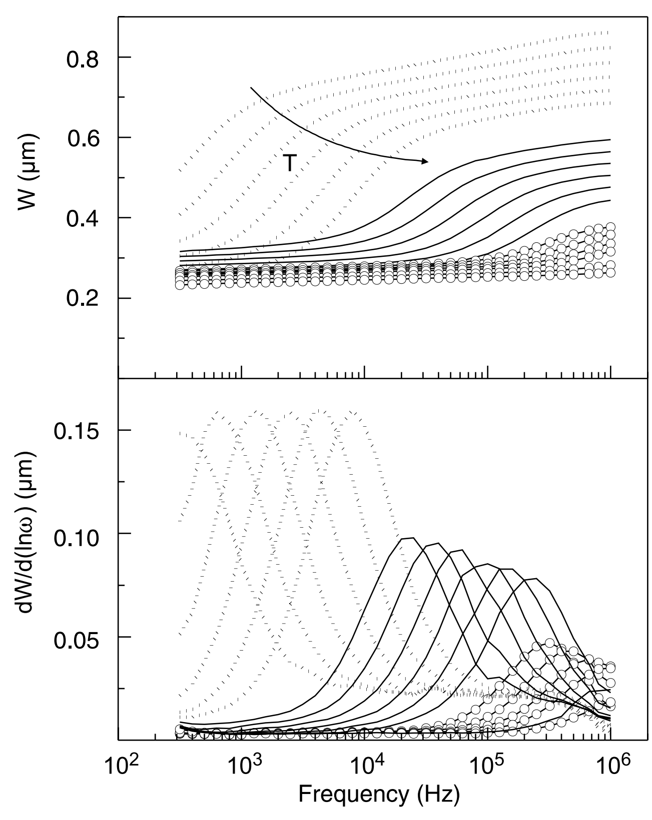

Fig. 5. Admittance spectra and their derivatives in the 180–230 K temperature range for sample in the relaxed state (continuous lines), after reverse-bias soaking (dotted lines), and after light soaking (circles).

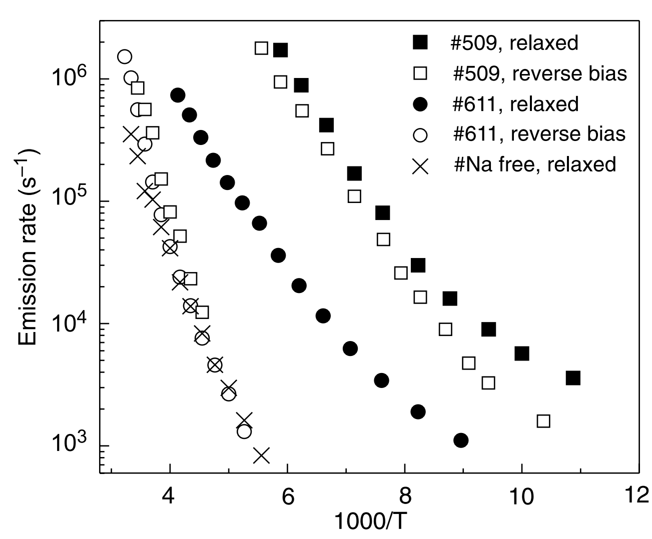

Fig. 6. Emission rates as a function of inverse temperature derived from admittance measurements for three samples in the relaxed and reverse bias-soaked state. In the sample #611 the 0.26 eV level is observed, which is replaced by emission from 0.34 eV level after reverse bias. In the 509 sample a level 0.19 eV is initially observed, while after reverse bias second level 0.34 eV appears. In the sample marked as Na-free (with sodium barrier) in the relaxed state only 0.34 eV level is observed.

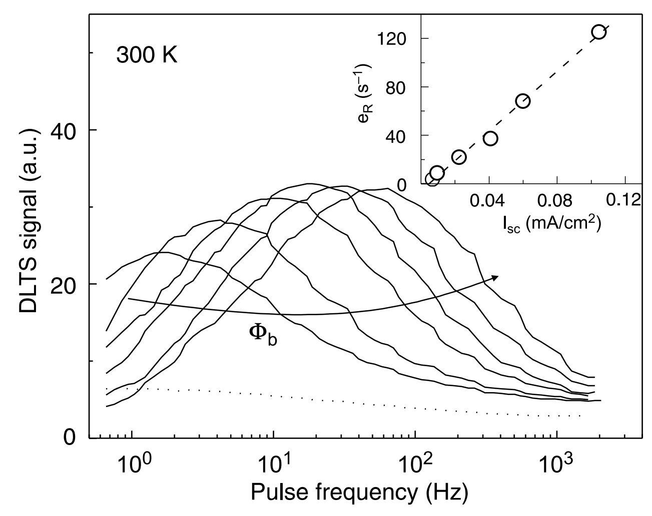

Fig. 7. DLTS frequency scan spectrum measured at room temperature when injection pulses are applied to the sample illuminated with blue light of increasing intensity Φ_b. The spectrum obtained in the dark is also shown as dotted line. In the insert, recombination rates derived from the positions of the DLTS maxima are plotted against the values of short circuit current measured at the same blue light intensities.

line devices. From the other side, it is known that injection produces a persistent increase in the junction capacitance due to electrons captured in some very deep states. From the annealing characteristics of the non-equilibrium negative charge introduced into the junction by illumination or forward bias we have deduced that these traps have to be deeper than 0.6 eV. Several experiments also revealed that in certain conditions the charge trapped in deep centres might be easily neutralized by "blue" light of energy exceeding the energy gap of the CdS buffer [4,20,21]. "Blue" light creates free holes in the buffer which are then swept to the absorber and might recombine with captured electrons. Thus, we have concluded that a deep level involved in the persistent changes of charge distribution within absorber might act as the recombination centre. Indeed, although injection pulses alone do not produce DLTS signal, a well-resolved peak appears, if the sample is simultaneously illuminated with blue light (490 nm interference filter) while injection pulses are applied [22]. Position of that peak does not depend on temperature, but on intensity of the blue light (Fig. 7.). We have concluded, that this peak is due to the recombination of injected and captured electrons with holes swept from the CdS buffer to the absorber. Assuming that recombination rate e_R is expressed by $e_R = pv_{th}\sigma_h$, we have calculated the capture cross section for holes for that electron trap $\sigma_h = 5\times10^{-14}$ cm^2. We have used free hole concentration p estimated from the value of the short circuit current I_{sc} measured at the same blue illumination intensity. High value of σ_h together with high concentration of the traps involved in that process (estimated to be at least equal to the net acceptor concentration $N_a = 2\times10^{16}$ cm^{-3}) support the conclusion, that this centre is a dominating recombination level in the CIGS absorber.

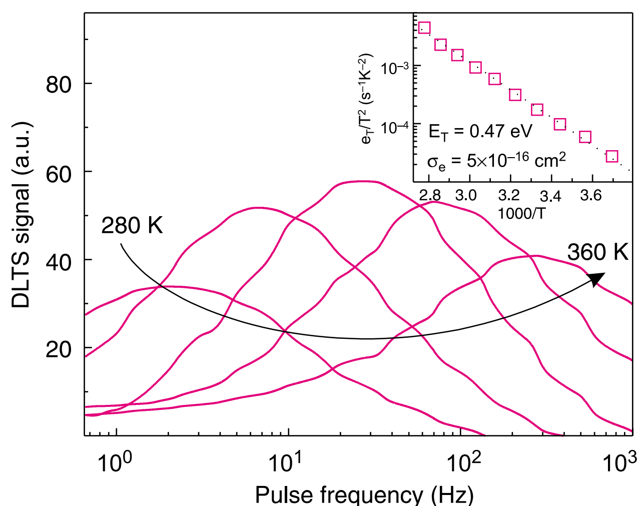

Fig. 8. DLTS frequency scan spectra obtained by use of injection pulses for the sample after accelerated aging test. In the insert Arrhenius plot for this level is shown.

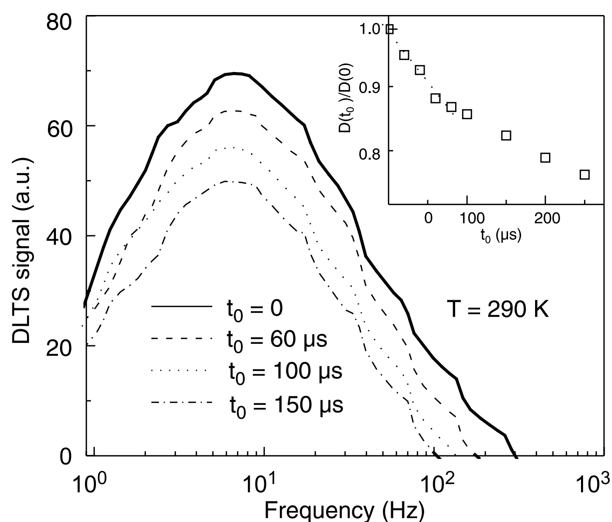

Fig. 9. The results of the double pulse experiment performed on the 0.47 eV electron trap. Second majority carrier pulse of length t_0 is applied after the injection pulse. In the insert a relative decrease of the DLTS signal is plotted in the semi-logarithmic scale vs. second pulse length.

We have tentatively assigned it to V_{Se} since according to theory this is a defect, which shows very strong coupling to the lattice, with a level close to the valence band (before relaxation) which moves close to the conduction band after relaxation. This feature would explain its involvement in the metastable phenomena.

The injection DLTS experiments have been performed also on the samples with inferior photovoltaic performance (e.g. after accelerating aging test) [22,23]. Deep electron bulk level of depth E_T = 0.47 eV has been revealed (Fig. 8.). On this trap level a double-pulse DLTS experiment has been performed in order to determine capture cross section for holes and thus estimate its activity as a recombination level [22]. In the double pulse method, an injection pulse is followed by a short majority carrier pulse of length t_o, during which some of the captured electrons recombine. The decrease in the DLTS signal, depending on t_o, is then observed and hence σ_h might be calculated by using a formula

$$\frac{D(t_o)}{D(0)} = \exp\{-t_o \sigma_h p\}. \tag{12}$$

The results are shown in Fig. 9. Very low hole capture cross section $\sigma_h \approx 10^{-18}$ cm^2 has been obtained, therefore we conclude that this electron trap is not an efficient recombination centre and thus cannot be responsible for the performance loss observed in the devices after accelerated aging test.

5. Conclusions

In this paper we have presented our results on the electronic properties of defect levels in Cu(In,Ga)Se$_2$ derived from capacitance spectroscopy. This work proves that capacitance methods are powerful tools for obtaining information on defect physics in the photovoltaic devices.

The electronic parameters of trap levels determined in our measurements are collected in Table 1. The assignment of levels to particular defects has been made by comparing experimental trap depths and electrical activities to the theoretical values of ionisation energies for intrinsic defects [19,24].

The results show, that levels due to In$_{Cu}$ antisite are a dominating feature of the DLTS and admittance spectra. This might be expected, as the composition of the CIGS layers in solar cells is slightly indium-rich.

Another important centre in CIGS is in our opinion the compensating donor V_{Se}. We have proposed that this is a defect responsible for the metastable phenomena and thus have profound influence on the charge and voltage distribution within the structure. It also seems to be an efficient recombination centre. Since current transport in the CIGS devices is dominated by recombination in the depleted region, V_{Se} centres might have significant impact on their photovoltaic performance. Therefore better control over selenium incorporation during growth of the absorber seems to be a very important issue.

Acknowledgements

The authors are grateful for cooperation and providing devices used in these studies to colleagues from Angstrom Solar Centre, Uppsala University and IPE, Stuttgart University. This work has been supported by grant KBN 05/T11/98.

References

1. M.A. Contreras, B. Egaas, K. Ramanathan, J. Hiltner, A. Swartzlander, F. Hasoon, and R. Noufi, "Progress toward 20% efficiency in Cu(In,Ga)Se$_2$ polycrystalline thin film solar cells", *Progr. Photov. Res. Appl.* **7**, 311–316 (1999).

© 2003 COSiW SEP, Warsaw

2. U. Rau and H.W. Schock, "Electronic properties of Cu(In,Ga)Se_2 heterojunction solar cells - recent achievements, current understanding, and future challenges" *Appl. Phys.* **A69**, 131–147 (1999).
3. M. Igalson and P. Zabierowski, "Transient capacitance spectroscopy of defect levels in CIGS devices", *Thin Solid Films* **361/362**, 371–377 (2000).
4. P. Zabierowski, U. Rau, and M. Igalson ,"Classification of the metastabilities in the electrical characteristics of ZnO/CdS/Cu(In,Ga)Se_2 devices", *Thin Solid Films* **387**, 147–150 (2001).
5. M. Igalson, M. Bodegard, L. Stolt, and A. Jasenek, "The "defected layer" and the mechanism of the interface-related metastable behaviour in the ZnO/CdS/Cu(In,Ga)Se_2 devices", *Thin Solid Films* **431/432C**, 153–157 (2003).
6. J. Kessler, M. Bodegård, J. Hedström, and L. Stolt, "Baseline Cu(In,Ga)Se_2 device production: control and statistical significance", *Sol. Ener. Mat. Sol. Cells* **67**, 67–75 (2001).
7. V. Nadenau, D. Branger. D. Hariskos, M. K. Kessler, D. Schmid, C. Köble, A. Oberacker, M. Ruck, U. Rühle, R. Schäfler, D. Schmid, T. Walter, S. Zweigart, and H.W. Schock, "Solar cells based on $CuInSe_2$ and related compounds: material and device properties and processing", *Progr. Photovolt. Res. Appl.* **3**, 363–382 (1995).
8. D.V. Lang, "Space charge spectroscopy in semiconductors", in *Thermaly Stimulated Relaxation in Solids*, pp. 93–133, edited by P. Braunlich, Springer-Verlag, 1979.
9. G.P. Li, K.L. Wang, "A novel technique for studying electric field effect of carrier emission from a deep level centre", *Appl. Phys. Lett* **42**, 838–840 (1983).
10. M. Igalson, P. Zabierowski, A. Romeo, L. Stolt, "Reverse –bias DLTS for investigation of the interface region of thin film solar cells", *Opto-Electron. Rev*. **8**, 346 –349 (2000).
11. L. Dobaczewski, P. Kaczor, I. D. Howkins, A. R. Peaker, "Laplace transform deep level spectroscopic studies of defects in semiconductors" *J. Appl. Phys.* **76**, 194-198 (1994).
12. P. Blood and J.W. Orton, *The Electrical Characterization of Semiconductors: Majority Carriers and Electron States*, London, Academic Press, 1990.
13. A. Niemegeers, M. Burgelman, R. Herberholz, U. Rau, D. Hariskos, H. W. Schock, "Model for electronic transport in Cu(In,Ga)Se_2 solar cell", *Prog. Photovolt. Res. Appl.* **6**, 407–421 (1998).
14. R. Herberholz, M. Igalson, and H.W. Schock, "Distinction between bulk and interface states in $CuInSe_2$/CdS/ZnO by space charge spectroscopy", *J. Appl. Phys.* **83**, 318–325 (1998).
15. P. Zabierowski, M. Igalson, and H.W. Schock, "Light-induced metastabilities in the interface region of Cu(In,Ga)Se_2--based photovoltaic devices studied by Laplace transform junction spectroscopy", *Solid State Phenomena* **67/68**, 403–408 (1999).
16. M. Igalson, A. Kubiaczyk, P. Zabierowski, M. Bodegård, and K. Granath, "Electrical characterization of ZnO/CdS/ /Cu(In,Ga)Se_2 devices with controlled sodium content", *Thin Solid Films* **387**, 225–227 (2001).
17. P Zabierowski and M. Igalson, "Thermally assisted tunnelling in Cu(In,Ga)Se_2-based photovoltaic devices", *Thin Solid Films* **361/362**, 268–272 (2000).
18. P. Zabierowski, *Ph. D. Thesis*, Warsaw University of Technology, Warszawa 2002.
19. S.B. Zhang, S.H. Wei, A. Zunger, and H. Katayama--Yoshida, "Defect physics of the $CuInSe_2$ chalcopyrite semoconductor", *Phys. Rev.* **B57**, 9642–9657 (1998).
20. M. Igalson and L. Stolt, "Deep levels and space-charge distribution in Cu(In,Ga)Se_2 photovoltaic devices", *Jap. J. Appl. Phys.* **39** suppl. 39-1, 426-429 (2000).
21. M. Igalson, M. Bodegard, and L. Stolt, "Reversible changes of the fill factor in the ZnO/CdS/Cu(In,Ga)Se_2 solar cells", *Sol. En. Mat & Sol. Cells* **80**, 195–207 (2003).
22. M. Igalson, M. BodegÍrd, and L. Stolt, "Recombination centres in the Cu(In,Ga)Se_2-based photovoltaic devices", *J. Phys. Chem. Solids* **64,** 2041–2045 (2003).
23. M. Igalson, M. Wimbor, and J. Wennerberg, "The change of the electronic properties of CIGS devices induced by the 'damp heat' treatment", *Thin Solid Films* **403/404**, 320–324 (2002).
24. S.H. Wei, S. B. Zhang, and A. Zunger, "Effects of Na on the electrical and structural properties of $CuInSe_2$" *J. Appl. Phys.* **85**, 7214–7218 (1999).

Institute of Physics Publishing

www.bookmarkphysics.iop.org.

Institute of Physics Publishing has added 14 new books to the sale list and slashed their prices. A further 27 books have been knocked down by 80% and even 90%.

Physical Methods for Materials Characterisation

P E J Flewitt, Magnox Electric, Berkeley, UK; R K Wild, University of Bristol, UK.

In the second edition of this popular text, the authors provide a comprehensive description of the range of techniques currently in use for the characterisation of the microstructure of materials.

Paperback **£37.50 US $59.99**

Next Generation Photovoltaics

Ed. Marti; A Luque, Institute of Solar Energy, University of Madrid, Spain.

Photovoltaics are regarded by many as the most likely candidate for long term sustainable energy production, yet their implementation has been restricted by the high costs involved. Nevertheless, the theoretical limit on photovoltaic energy conversion efficiency, above 85%, suggests that there is room for substantial improvement of present commercially available solar cells, both silicon and thin-film based. Current research efforts are focused on implementing novel concepts to produce a new generation of low-cost, high-performance photovoltaics that make improved use of the solar spectrum.

Hardback **£85.00 US $125.00**

Stimulated Brillouin Scattering

M Damzen; V I Vlad; V Mocofanescu, Imperial College London and University of Bucharest, Romania.

Stimulated Brillouin Scattering (SBS) is the most important example of a stimulated scattering process; light scattering which occurs when the intensity of the light field itself affects the propagating medium. A phenomenon which has been known of for some 35 years in solid state laser research, it has recently become relevant in the optical fibre industry, due to the increasing intensity required in optical fibre cores (and their long interaction lengths). SBS is one of the major limiting factors on the amount of power that can be transmitted via an optical fibre.

Hardback **£60.00 US $95.00**

Theory of Superconductivity

A S Alexandrov, Quantum Structures and Phase Transitions Group, Loughborough University, UK.

Theory of Superconductivity leads the reader from basic principles through detailed derivations to a description of the many interesting phenomena in conventional and high-temperature superconductors. Physical properties of novel superconductors, in particular the normal state, superconducting critical temperatures and critical fields, isotope effects, normal and superconducting gaps, tunnelling, angle-resolved photoemission, stripes and symmetries are described in a self-consistent fashion.

Hardback **£65.00 US $100.00**

The Magnetocaloric Effect and its Applications

A M Tishin, Physics Faculty, M V Lomonosov Moscow State University, Russia; Y I Spichkin, Head of Research and Development, Advanced Magnetic Technologies and Consulting Ltd., Russia.

The magnetocaloric effect describes the change in temperature of a magnetic material under adiabatic conditions through the application or removal of an external magnetic field. This effect is particularly pronounced at temperatures and fields corresponding to magnetic phase transitions, and it is a powerful and widely used tool for investigation of the magnetic state and mechanisms of these transitions. More recently there has been significant interest in its possible exploitation in magnetic refrigeration and cryocooling systems.

Hardback **£90.00 US $135.00**

Astrophysical Techniques

C R Kitchin, University of Hertfordshire, UK.

This new edition of Professor Kitchin's popular Astrophysical Techniques retains the aims of the earlier edition in providing a comprehensive and clearly understandable account of the instruments and techniques used in modern astronomy and astrophysics. Many new instruments and techniques are included for the first time, and some topics have been eliminated on the grounds that they have not been used by either professional or amateur astronomers for many years.

Paperback **£35.00 US $55.00**

© 2003 COSiW SEP, Warsaw